Title
Homotopy Directed Optimization to Design a Six-Bar Linkage for a Lower Limb With a Natural Ankle Trajectory

Journal
Journal of Mechanisms and Robotics, 8(6)

ISSN
1942-4302

Authors
Tsuge, Brandon Y
Plecnik, Mark M
McCarthy, J Michael

Publication Date
2016-12-01

DOI
10.1115/1.4034141

Peer reviewed

Homotopy Directed Optimization to Design a Six-Bar Linkage for a Lower Limb with a Natural Ankle Trajectory

Brandon Y. Tsuge
Graduate Student Researcher
Email: btsuge@uci.edu

Mark M. Plecnik
Post-Doctoral Researcher
Email: mplecnik@uci.edu

J. Michael McCarthy
Professor, ASME Fellow
Email: jmmccart@uci.edu

Robotics and Automation Laboratory
Department of Mechanical and Aerospace Engineering
University of California, Irvine
Irvine, California 92697

This paper presents a synthesis method for the Stephenson III six-bar linkage that combines the direct solution of the synthesis equations with an optimization strategy to achieve increased performance for path generation. The path synthesis equations for a six-bar linkage can reach as many as 15 points on a curve, however, the degree of the polynomial system is 10^{46}*. In order to increase the number of accuracy points and decrease the complexity of the synthesis equations, a new formulation is used that combines 11 point synthesis with optimization techniques to obtain a six-bar linkage that minimizes the distance to 30 accuracy points. This homotopy directed optimization technique is demonstrated by obtaining a Stephenson III six-bar linkage that achieve a specified gait trajectory.*

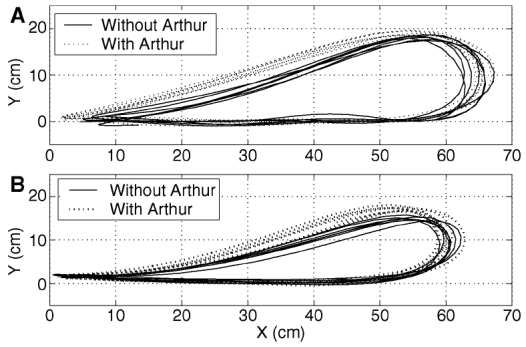

Fig. 1: The ankle trajectories achieved by the ARTHuR Step Robot, [1].

1 Introduction

In this paper, we present a new synthesis procedure that combines homotopy solution to the 11-point the path synthesis equations for a Stephenson III six-bar linkage with an optimization strategy that allows the increase of the number of accuracy points to 30 and more. This research is motivated both by the goal to achieve a design methodology for linkages with increasingly complex synthesis equations, as well as to obtain a linkage that matches the gait trajectory of a human ankle to act as an exoskeleton for rehabilitative treadmill training.

2 Literature review

Robotic rehabilitation for human walking movements uses a mechanical system to guide a patient during treadmill walking exercises. For example, the ARTHuR system provides two actuators that guide a patient's ankle through a stepping movement on a treadmill, [1]. The angle trajectories achieved with and without the ARTHuR system are shown in Figure 1.

It is known that single degree-of-freedom linkage systems can trace complex planar curves like the ankle trajectory in Figure 1. A theoretical result by A. B. Kempe [2], which has been strengthened recently [3], states that any plane algebraic curve has an associated linkage that can trace the curve. Also see Artobolevskii [4] for linkages that generate specialized plane curves.

Our goal is a design procedure for a six-bar linkage that can trace human ankle trajectories, such as those provided to us from the Human Interactive Robotics Lab under the di-

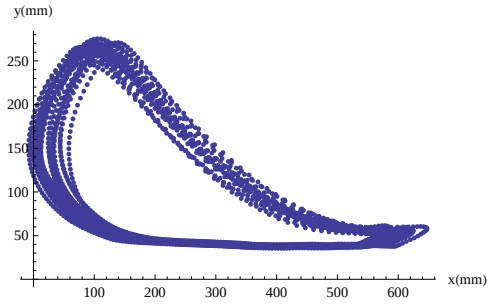

Fig. 2: Coordinates of the ankle during multiple gait cycles

rection of Prof. Nina Robson at California State University, Fullerton, Figure 2. The synthesis equations for the six-bar path generator were derived by Kim et al. [5], who show that this linkage can be designed to pass its coupler curve through 15 points. In this paper, we present an alternative derivation for these equations and obtain 154 quadratic equations in 154 unknowns. This shows there can be as many as 2^{154}, or approximately 10^{46}, solutions.

As far as we can tell, there has been no attempt at a direct solution of the 15-point path generation synthesis equations for the six-bar linkage. Path synthesis of six-bar linkages have relied on optimization techniques beginning with Bhatia and Bagci [6]. Nolle [7] and Root and Ragsdell [8] provide an overview of the use of optimization methods in linkage design. For a recent example, see Mehdigholi [9]. As Nolle points out, linkage design equations have a large number of local minima, which makes the result dependent upon initial choices for the design parameters.

In order to avoid local minima, modern direct search strategies start with a random population of design parameter vectors and then provide a systematic way to modify these parameter vectors to find new designs [10]. Bulatovic and Dordevic [11] applied the technique of Differential Evolution to the design a six-bar Stephenson III path generator that fit 32 points on a specified curve. Bulatovic et al [12] used the Cuckoo Search algorithm to design a Stephenson III six-bar with a coupler curve that has 26 specified points divided between two circular dwells. The Cuckoo Search algorithm is an example of a direct search strategy that uses a nature-based heuristic to combine design parameter vectors to find new designs. Other examples of these heuristics include simulated annealing used by Dibakar and Mruthyunjaya [13] to design two degree-of-freedom planar linkage systems, the particle swarm method used by McDougall and Nokleby [14] to design four-bar linkages, and the ant search algorithm used by Xiao and Tao [15] and by Smaili and Diab [16] to design four-bar path generators.

In this paper, rather than use a direct search optimizer that randomly selects the initial parameter vectors, we solve for the path-generator design equations for 11 specified points on the desired path using a homotopy solver [17]. These solutions are then used as the initial design parameter vectors that are used in a gradient optimizer to fit 60 specified points on the path. We call this combination of homotopy generated exact solutions with gradient optimization, *homotopy directed optimization*.

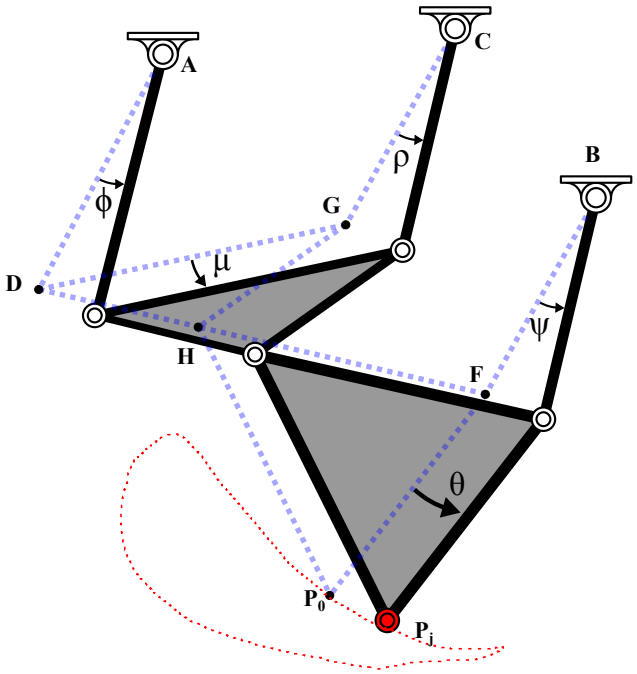

Fig. 3: Stephenson III six-bar linkage

3 Stephenson III Path Synthesis Equations

A Stephenson III six-bar linkage is shown in Figure (3). The seven hinged joints of this linkage are denoted by the complex vectors, A, B, C, D, F, G and H. the point P is the point that is to trace the coupler curve. The coordinates of the joints in the reference position are the design parameters that are to be determined by the synthesis process. The angles ψ, ρ, ϕ, μ, and θ are measured from the reference position to the current configuration.

Path synthesis begins with the specification of a set of N points, P_j, $j = 0, \ldots, N-1$ that define the desired coupler curve for the Stephenson III six-bar linkage. In the reference position, we have the three loop equations,

$$\begin{aligned}
&(F-B)+(P_0-F) = P_0-B,\\
&(G-C)+(H-G)+(P_0-H) = P_0-C,\\
&(D-A)+(H-D)+P_0-H) = P_0-A.
\end{aligned} \tag{1}$$

For convenience introduce the notation,

$$\begin{aligned}
&Q_j = e^{i\phi_j} \qquad R_j = e^{i\rho_j} \qquad S_j = e^{i\psi_j}\\
&T_j = e^{i\theta_j} \qquad U_j = e^{i\mu_j} \qquad j = 1, \ldots, N-1,
\end{aligned} \tag{2}$$

to represent the rotation of the individual links of the six-bar linkage. These parameters satisfy the normality conditions,

$$\begin{aligned}
&Q_j\bar{Q}_j = 1, \qquad R_j\bar{R}_j = 1, \qquad S_j\bar{S}_j = 1,\\
&T_j\bar{T}_j = 1, \qquad U_j\bar{U}_j = 1, \qquad j = 1, \ldots, N-1,
\end{aligned} \tag{3}$$

where the star denotes the complex conjugate.

Thus, for the remaining coupler points P_j, $j = 1,\ldots,N-1$, we have the loop equations,

$$\begin{aligned}
&Q_j(D-A)+U_j(H-D)+T_j(P_0-H) = P_j-A\\
&R_j(G-C)+U_j(H-G)+T_j(P_0-H) = P_j-C\\
&S_j(F-B)+T_j(P_0-F) = P_j-B\\
&j = 1,\ldots,N-1.
\end{aligned} \tag{4}$$

In addition, we have the complex conjugate loop equations,

$$\begin{aligned}
&\bar{Q}_j(\bar{D}-\bar{A})+\bar{U}_j(\bar{H}-\bar{D})+\bar{T}_j(\bar{P}_0-\bar{H}) = \bar{P}_j-\bar{A}\\
&\bar{R}_j(\bar{G}-\bar{C})+\bar{U}_j(\bar{H}-\bar{G})+\bar{T}_j(\bar{P}_0-\bar{H}) = \bar{P}_j-\bar{C}\\
&\bar{S}_j(\bar{F}-\bar{B})+\bar{T}_j(\bar{P}_0-\bar{F}) = \bar{P}_j-\bar{B}\\
&j = 1,\ldots,N-1.
\end{aligned} \tag{5}$$

Equations 4, 5, and 3 form the synthesis equations for the Stephenson III path generator. Notice that for N specified path points, we have seven complex vector joint unknowns, five joint angle unknowns in $N-1$ task positions, together their complex conjugates, for a total of $14+10*(N-1))$ unknowns. And we have three complex loop equations and their conjugates, as well as five normality conditions in the $N-1$ task positions, for a total of $11*(N-1)$ equations. Thus, we have as many equations a unknowns for the case N=15, which yields 154 quadratic equations in 154 unknowns.

The challenge posed by the solution of these synthesis equations can be estimated by computing the Bezout root count [17], which is $d = 2^{154}$ or 2.28×10^{46}.

4 11-Point Path Synthesis

In order to reduce the complexity of the synthesis equations for a Stephenson III path generator, we specify the dimensions and the $n-1$ positions of the RR chain BFP_j, $j = 1,\ldots,N-1$, which reduces the specified number points on the curve to $N = 11$—recall that R denotes a revolute, or hinged joint. This simplifies equations (4), (5), and (3) into the following two sets,

$$\begin{aligned}
\mathcal{S}_1:\quad &S_j(F-B)+T_j(P_0-F) = P_j-B,\\
&\bar{S}_j(\bar{F}-\bar{B})+\bar{T}_j(\bar{P}_0-\bar{F}) = \bar{P}_j-\bar{B},\\
&S_j\bar{S}_j = 1,\\
&T_j\bar{T}_j = 1, \qquad\qquad j = 1,\ldots,10.
\end{aligned} \tag{6}$$

and

$$\begin{aligned}
\mathcal{S}_2:\quad &Q_j(D-A)+U_j(H-D)+T_j(P_0-H) = P_j-A,\\
&R_j(G-C)+U_j(H-G)+T_j(P_0-H) = P_j-C,\\
&\bar{Q}_j(\bar{D}-\bar{A})+\bar{U}_j(\bar{H}-\bar{D})+\bar{T}_j(\bar{P}_0-\bar{H}) = \bar{P}_j-\bar{A},\\
&\bar{R}_j(\bar{G}-\bar{C})+\bar{U}_j(\bar{H}-\bar{G})+\bar{T}_j(\bar{P}_0-\bar{H}) = \bar{P}_j-\bar{C},\\
&Q_j\bar{Q}_j = 1,\\
&R_j\bar{R}_j = 1,\\
&U_j\bar{U}_j = 1, \qquad\qquad j = 1,\ldots,10.
\end{aligned} \tag{7}$$

The equations in $\mathcal{S}_1$ can be solved to determine unknowns S, $\bar{S}$, T, $\bar{T}$. This computing S and $\bar{S}$ from the first equations, and substituting the result into the normalization conditions $S\bar{S} = 1$, to obtain,

$$aT_j+b+c\bar{T}_j = 0, \quad j = 1,\ldots,10, \tag{8}$$

where

$$\begin{aligned}
&a = (\bar{P}_j-\bar{B})(P_0-F),\\
&b = (F-B)(\bar{F}-\bar{B})-(P_j-B)(\bar{P}_j-\bar{B})-(P_0-F)(\bar{P}_0-\bar{F}),\\
&c = (P_j-B)(\bar{P}_0-\bar{F}).
\end{aligned} \tag{9}$$

Multiply (8) by T_j to obtain a quadratic equation, which is solved using the quadratic formula. And, the values for S, $\bar{S}$, $\bar{T}$ are found by back substitution.

Once equations $\mathcal{S}_1$ are solved, equations $\mathcal{S}_2$ have the unknowns $A, C, D, G, H, Q_j, R_j, U_j$ and their conjugates. Thus, for the case of $N = 11$, the path synthesis equations reduce to 70 quadratic equations in 70 unknowns. The degree of this system is 2^{70}.

This system of equations has been studied by Plecnik and McCarthy [18, 19], who show that it has the multi-homogeneous degree, $d = 264,241,152$. And they obtain a parameter homotopy for the solution of the 11-point path synthesis equations for a given RR chain. In what follows, we use this parameter homotopy to generate the initial design parameter vectors for the optimization step.

5 Optimization

Once a set of initial design parameter vectors are determined by the homotopy solution of the 11-point synthesis equations, a gradient optimizer is used to minimize the distance of the resulting linkage to the specified points, P_k, $k = 0,\ldots,N_P-1$, on the desired coupler curve. Recall that the RR chain BFP_k is specified and the system of equations $\mathcal{S}_1$ can be solved for S_k and T_k, which define the joint angles ψ_k and θ_k.

If the point P_k is on the coupler curve of Stephenson III linkage formed by RR chain BFP_k and the remaining design parameters, $\mathbf{r} = (A,C,D,G,H)$, then they satisfy the loop

equations defined by $\mathcal{S}_2$, that is

$$
\begin{aligned}
&Q_k(D-A) = -U_k(H-D) - T_k(P_0-H) + (P_k-A),\\
&\bar{Q}_k(\bar{D}-\bar{A}) = -\bar{U}_k(\bar{H}-\bar{D}) - \bar{T}_k(\bar{P}_0-\bar{H}) + (\bar{P}_k-\bar{A}),\\
&R_k(G-C) = -U_k(H-G) - T_k(P_0-H) + (P_k-C),\\
&\bar{R}_k(\bar{G}-\bar{C}) = -\bar{U}_k(\bar{H}-\bar{G}) - \bar{T}_k(\bar{P}_0-\bar{H}) + (\bar{P}_k-\bar{C}),\\
&k = 1,\ldots,N_P-1. \qquad (10)
\end{aligned}
$$

Eliminate Q_k and R_k by multiplying the complex conjugate equations to obtain,

$$
\begin{aligned}
&|D-A|^2 = |U_k(H-D) + T_k(P_0-H) - (P_k-A)|^2,\\
&|G-C|^2 = |U_k(H-G) + T_k(P_0-H) - (P_k-C)|^2,\\
&k = 1,\ldots,N_P-1. \qquad (11)
\end{aligned}
$$

This is k sets of two linear equations in the two unknowns joint angles U_k and $\bar{U}_k$.

In order to solve these equations, it is convenient to introduce the parameters,

$$
\begin{aligned}
&a = a_x + ia_y = H - D\\
&b_k = b_{xk} + ib_{yk} = T_k(P_0-H) - P_k + A\\
&c = c_x + ic_y = H - G\\
&d_k = d_{xk} + id_{yk} = T_k(P_0-H) - P_k + C\\
&f = f_x + if_y = D - A\\
&g = g_x + ig_y = G - C, \qquad (12)
\end{aligned}
$$

which can be determined from the six-bar linkage defined by the RR chain BFP_0 and the design vector $\mathbf{r} = (A,C,D,G,H)$. to obtain k sets of two equations in the two unknowns U_k and $\bar{U}_k$,

Substitute the parameters (12) into (11) to obtain,

$$
\begin{aligned}
&U_k a\bar{b}_k + \bar{U}_k \bar{a} b_k = f\bar{f} - a\bar{a} - b_k\bar{b}_k,\\
&U_k c\bar{d}_k + \bar{U}_k \bar{c} d_k = g\bar{g} - c\bar{c} - d_k\bar{d}_k, \quad k = 1,\ldots,N_P-1. \qquad (13)
\end{aligned}
$$

Each of which can be solved to obtain,

$$
\begin{aligned}
&U_k = \frac{\begin{vmatrix} f\bar{f} - a\bar{a} - b_k\bar{b}_k & \bar{a}b_k \\ g\bar{g} - c\bar{c} - d_k\bar{d}_k & \bar{c}d_k \end{vmatrix}}{\begin{vmatrix} a\bar{b}_k & \bar{a}b_k \\ c\bar{d}_k & \bar{c}d_k \end{vmatrix}}, \bar{U}_k = \frac{\begin{vmatrix} a\bar{b}_k & f\bar{f} - a\bar{a} - b_k\bar{b}_k \\ c\bar{d}_k & g\bar{g} - c\bar{c} - d_k\bar{d}_k \end{vmatrix}}{\begin{vmatrix} a\bar{b}_k & \bar{a}b_k \\ c\bar{d}_k & \bar{c}d_k \end{vmatrix}},\\
&k = 1,\ldots,N_P-1. \qquad (14)
\end{aligned}
$$

The parameters U_k and $\bar{U}_k$ satisfy the normality condition, $U_k\bar{U}_k = 1$, when P_k is on the coupler curve of the linkage defined by the design parameter vector $\mathbf{r} = (A,C,D,G,H)$. We use these this to construct the objective function,

$$
F(\mathbf{r}) = \sum_{i=1}^{N_P-1} U_k\bar{U}_k - 1 = \sum_{i=1}^{N_P-1} \sin^2\mu_k + \cos^2\mu_k - 1, \qquad (15)
$$

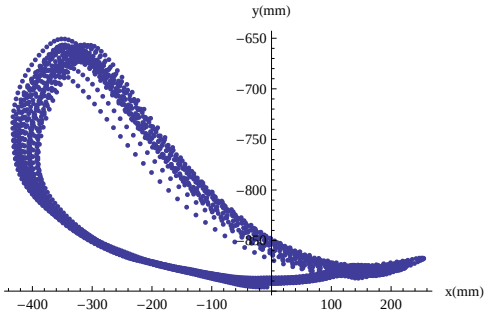

Fig. 4: Coordinates of the ankle relative to the hip joint

which measures the error between the set of points P_k, $k = 0,\ldots,N_P-1$ and the coupler curve traced by the six-bar linkage formed by the RR chain BFP_0 and the design vector $\mathbf{r} = (A,C,D,G,H)$.

6 Selection of Precision Points

The precision points, P_j and P_0, that are used in the path synthesis algorithm are derived from a set of data points collected from motion capture data of a walking subject. This data set marks the joint locations through 14 gait cycles as shown in figure 2. From this data, the lengths of the upper leg, lower leg, and foot can be determined. These lengths are determined by measuring the distances between the hip and knee, knee and ankle, and ankle and toe data points respectively. The motion capture data collected was in three dimensions, but only data in two dimensions was used in this procedure for simplicity. These points, however, were collected in the global frame, where the hip joint are moving. Since, the synthesis procedures require that the hip joint be stationary, a new set of data points relative to the hip is required. The coordinates of the ankle trajectory relative to the hip joint is shown in figure (4); the location of the hip joint was also moved to the origin for simplicity.

Next, one of the cycles was chosen to be the desired path for the synthesis procedure, as shown in figure (5). This path consisted of 205 data points. Since 205 data points could potentially create a minimization problem that will be too great in complexity, a reduction in the number of precision points is required. This was done by creating a basis spline equation for the 205 data points. This is a parametric equation and the data points are used as the control points.

Parametric equations for splines are constructed from *basis equations*, as shown in equations 16 and 17, where t is the parameter of the curve, k is the order of the curve, i is the ith control point, and $\mathbf{x}_i$ are elements of the knot vector. The knot vector deals with the weighting of a particular control point, as explained in [20].

$$
N_{i,1}(t) = \begin{cases} 1 & \text{if } \mathbf{x}_i \le t < \mathbf{x}_{i+1} \\ 0 & \text{otherwise.} \end{cases} \qquad (16)
$$

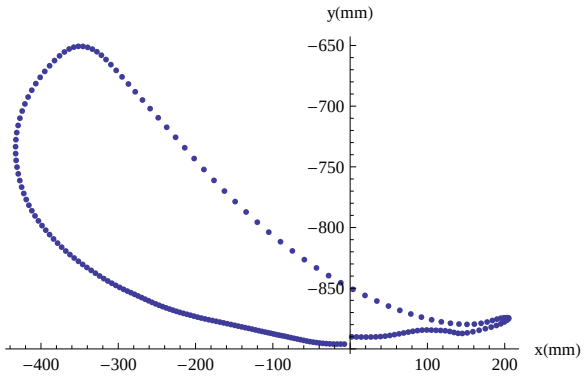

Fig. 5: Ankle trajectory of a single gait cycle relative to the hip joint

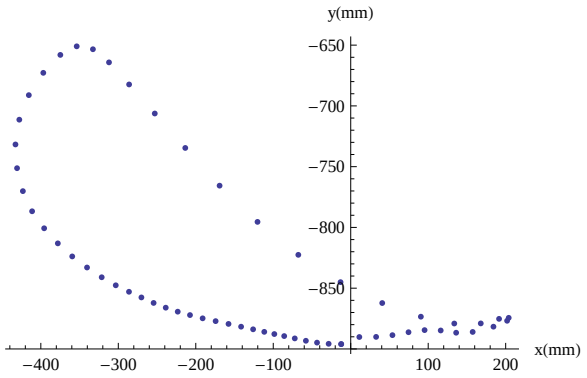

Fig. 6: Set of 60 precision points derived from a basis spline

$$N_{i,k}(t) = \frac{(t-\mathbf{x}_i)N_{i,k-1}(t)}{\mathbf{x}_{i+k-1}-\mathbf{x}_i} + \frac{(\mathbf{x}_{i+k}-t)N_{i+1,k-1}(t)}{\mathbf{x}_{i+k}-\mathbf{x}_{i+1}} \quad (17)$$

These basis equations are then used to form the parametric equations for the coordinates of the basis spline curve evaluated at t_j, where $\{P_x(t_j), P_y(t_j)\}$ is the jth point along the curve. Equations 18 and 19 are the parametric equations that yield the coordinates of the spline curve for a given parameter t.

$$P_x(t_j) = \sum_{i=0}^{n-1} P_{x,i}N_{i,k}(t_j) \quad (18)$$

$$P_y(t_j) = \sum_{i=0}^{n-1} P_{y,i}N_{i,k}(t_j) \quad (19)$$

Note that $\{P_{x,i}, P_{y,i}\}$ are retrieved from motion capture data and $\{P_x(t_j), P_y(t_j)\}$ are points along a continuous spline. The 205 data points of the ankle trajectory can then be used as the control points in the B-spline equation so that the ankle trajectory can be represented by a single parametric equation. Sixty values of t, between 0 and 1, were selected and substituted into the B-spline equations; these values of t were evenly distributed. The results define a number of points that are distributed about the curve.

From equations 16 and 17, it can be seen that the spline is a parametric equation in terms of the parameter t; this parameter varies from 0 to 1. There were 60 values of t that were evenly distributed between 0 and 1. The basis spline equation was then evaluated at each of these values, resulting in a set of 60 precision points displayed in table 1. The precision points used for the first gait cycle are in figure (6).

Lastly, the angle θ_j is the relative angle of the most distal link. Since the location of every point P and the lengths of links BF and FP are known from the spline equation and motion capture data respectively, θ_j can be determined by solving for the angle between two vectors. These values are also substituted in equation 15. The lengths of the upper leg, **BF**, and the lower leg, **FP**, are 397.874mm and 502.599mm respectively. The values of θ_j are listed in table 1.

6.1 Selection of Starting Linkage Solutions

In order to minimize equation 15 using the built-in minimization algorithms of *Mathematica*, starting values for the unknown variables are required. These unknown variables are the joint parameters, $\mathbf{A}, \mathbf{B}, \mathbf{C}, \mathbf{D}, \mathbf{F}, \mathbf{G}$, and $\mathbf{H}$. In order to choose these values we follow the method given in [18].

For this procedure, it is required that a 2R serial chain and 11 precision points are defined. The starting 2R chain is determined from the initial motion capture data. This 2R chain is **BFP**, from figure (3). For this particular problem, fixed pivot **B** was set to be at the origin. The lengths of the proximal and distal links were set to 397.874mm and 502.599mm respectively. These links match the lengths of the upper and lower leg segments of the user. These ultimately will be the leg segments of the exoskeleton that attach to the user. In addition, the 11 precision points that were used were selected by utilizing the basis spline method from the previous section. However, the only difference is that 11 evenly distributed values of the parameter t were used. The resulting precision points are shown in table 2 and plotted in figure (7). The calculations were carried out on Bertini on a Mac Pro machine. This machine had two 6-core Intel Xeon processors, for a total of 12 cores. The processor speed was 2.93GHz. The calculations were completed in 9.6 hours. The results showed that there were no linkages found that went through all positions. However, there were 13 linkages that went through 10 positions, 35 linkages that went through 9 positions, 183 linkages that went through 8 positions, 771 linkages that went through 7 positions, and 1445 linkages that went through 6 positions. All of these linkages were assembled into a single solution set. After duplicates were removed, there were a total of 2003 solutions. These linkage solutions were used as the starting linkages for the optimization procedure, explained in the next section. One of these linkages is shown in figure (8).

Table 1: Table of Data to be Substituted into the Error Function

j	$P_x(mm)$	$P_y(mm)$	$\theta(^\circ)$	j	$P_x(mm)$	$P_y(mm)$	$\theta(^\circ)$
0	-12.3013	-896.019	-	30	-415.486	-691.147	-48.4832
1	-28.5017	-895.762	-0.971	31	-396.802	-672.793	-50.9351
2	-43.4905	-894.79	-2.1413	32	-374.806	-658.035	-52.5427
3	-57.875	-893.271	-3.44411	33	-353.679	-650.984	-52.9764
4	-72.2304	-891.319	-4.82172	34	-332.749	-653.38	-52.155
5	-85.8676	-889.402	-6.03246	35	-311.995	-664.185	-50.2745
6	-98.6012	-887.739	-7.00875	36	-286.041	-682.357	-47.2952
7	-111.58	-885.925	-7.97049	37	-252.92	-706.259	-43.2771
8	-125.994	-883.837	-8.97115	38	-213.557	-734.6	-38.3101
9	-141.499	-881.686	-9.88991	39	-169.259	-765.635	-32.5368
10	-157.736	-879.401	-10.7333	40	-120.308	-795.439	-26.3087
11	-174.374	-877.111	-11.4156	41	-67.6423	-822.553	-19.7073
12	-191.139	-874.8	-11.9071	42	-13.1429	-845.034	-12.9489
13	-207.465	-872.119	-12.3876	43	40.66343	-862.223	-6.16035
14	-223.279	-869.328	-12.7076	44	90.53694	-873.455	0.3723
15	-238.762	-866.04	-13.1053	45	133.6625	-879.072	6.379523
16	-254.421	-862.136	-13.653	46	167.8554	-878.98	10.93037
17	-270.165	-857.609	-14.4337	47	191.4646	-875.24	13.03164
18	-286.202	-852.95	-14.8715	48	203.9151	-874.392	15.04815
19	-303.278	-847.622	-15.0286	49	201.845	-876.813	16.72373
20	-321.419	-841.008	-15.9984	50	184.2357	-881.676	17.61205
21	-340.361	-832.977	-18.3419	51	157.4071	-886.006	14.03234
22	-359.46	-823.865	-20.8059	52	136.0794	-886.649	10.07707
23	-378.044	-813.112	-23.794	53	116.143	-884.797	6.455648
24	-395.699	-800.707	-26.9922	54	95.34059	-884.501	4.048268
25	-411.249	-786.708	-30.3709	55	74.59698	-886.229	2.612696
26	-423.17	-770.139	-34.1777	56	53.85323	-888.645	1.604831
27	-430.681	-751.253	-38.1308	57	32.76674	-890.073	0.397363
28	-432.729	-731.726	-41.837	58	11.10905	-890.172	-1.16092
29	-427.766	-711.349	-45.3618	59	-12.3013	-896.019	0

6.2 Minimization Procedure and Results

Minimization of equation 15 for 60 precision points was carried out for each of the starting linkages from the previous section. The minimization problem, for each starting linkage, was completed using *Mathematica*'s built-in optimization algorithms. Six separate methods were used with the starting linkages and objective function. The algorithms options used were "ConjugateGradient" with "FletcherReeves," "Newton," "Gradient," "ConjugateGradient," "InteriorPoint," and "QuasiNewton."

Minimizing the objective function for 2003 different starting linkages with 6 different algorithms resulted in a large solution set that was to be sorted. Solutions with an error value greater than 3 were then were deemed to be undesirable linkages. Also, linkage solutions that a link length sum greater than 3000 were removed for the set. This was done in order to remove solutions that had a links that were too larger to be feasible.

The solutions that had branch defects were omitted. What remained where 6 linkages that were all in a single cluster; two linkages are considered to be in the same cluster if the norm of their differences was small. For the case of these 6 solutions, the norm of the differences of the joint coordinates were all less than one. This indicates that these solutions are essentially the same linkage. The 6 linkages solutions that were all found from the same starting linkage for each of the *Mathematica* functions. This starting linkage is shown in figure (8) and table 3. This solution is shown in figure (9) and the joint positions are in table 4. Figures (9(a)) and (9(b)) show two of the final linkage solutions with the largest variances. The norm of the differences between their joint coordinates was 1.02×10^{-5}.

Table 2: Table of the 11 Starting Precision Points for the Exact Six-Bar Synthesis Problem

P_x (mm)	P_y (mm)
-12.3013	-896.019
-90.5576	-888.832
-169.812	-877.728
-255.853	-861.74
-349.07	-828.994
-429.677	-754.752
-370.822	-656.01
-232.084	-721.162
35.88979	-860.879
204.9527	-874.624
102.895	-884.484

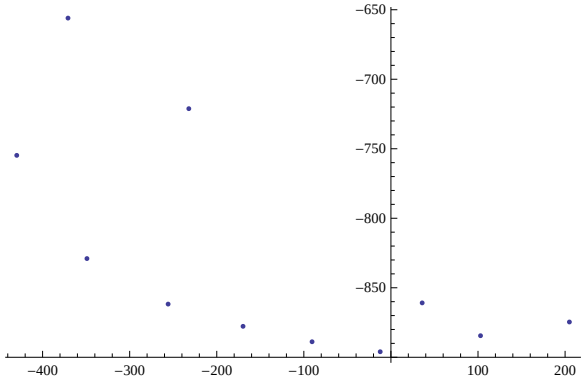

Fig. 7: Plot of the 11 starting precision points for the exact six-bar synthesis problem

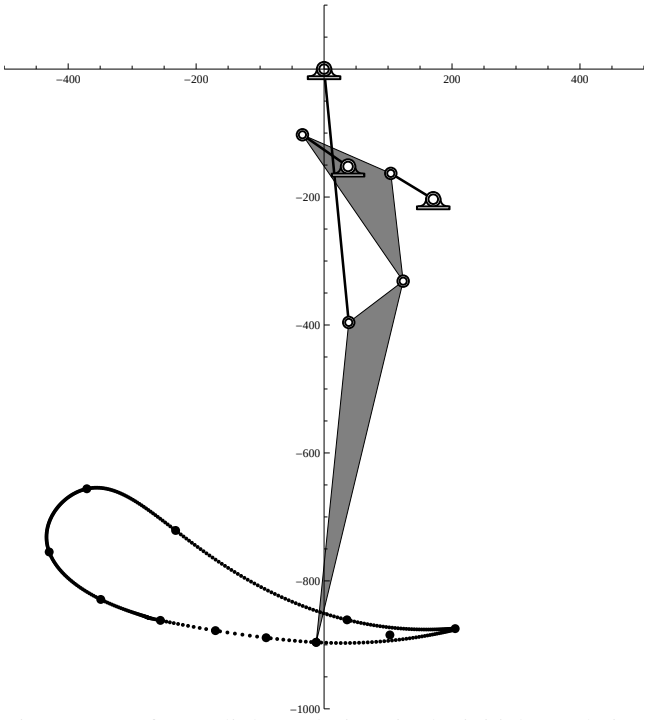

Fig. 8: One of 2003 linkage designs in the initial population positioned at the first precision point.

Table 3: Fixed Frame Joint Locations of the Starting Six-Bar Linkage at the first Precision Point

Joint	x-coordinate	y-coordinate
A	170.654	-203.351
B	0	0
C	37.497	-152.75
D	104.318	-163.023
F	38.571	369
G	123.619	-331.443
$\mathbf{P_0}$	-12.301	-896.019

Table 4: Linkage solution resulting from the minimization problem.

Error	2.472861
A_x	170.6508
A_y	-203.351
B_x	0
B_y	0
C_x	37.49712
C_y	-152.175
D_x	104.3177
D_y	-163.023
F_x	38.57078
F_y	-396
G_x	-33.817
G_y	-102.676
H_x	123.6186
H_y	-331.443

Lastly, it is shown in figure (10) that the optimized linkage solution moves through a desirable trajectory, however, there is a slight hyper-extension of the knee joint.

The Solidworks model with the graphed couple curve is shown in figure (11).

7 Conclusion

In this paper, a Stephenson III six-bar linkage path synthesis procedure that was specific to the design of a human walking linkage exoskeleton was presented. The procedure consisted of developing an error function based on three loop equations and relative angles. A reduction of variables occurred after using the dot product operation and the precision points were acquired from motion capture data and the use of basis spline equations. The starting values were determined by finding a six-bar linkage solution for the 11 point problem and the objective function was minimized using six of the built in Mathematica optimization functions. Precision points for both the 11 point problem and the optimization problem were both chosen by using basis splines. The basis splines were required because of the large amount of infor-

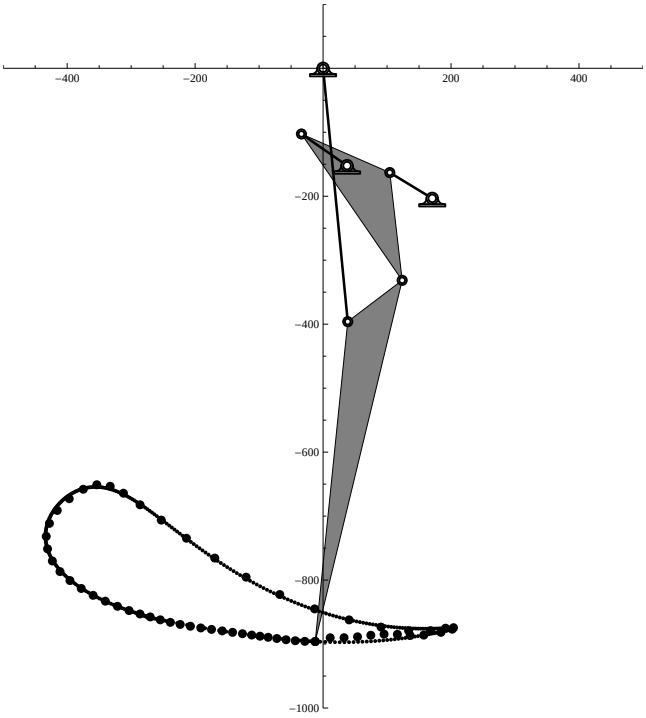

(a) Optimized linkage solution at the first precision point

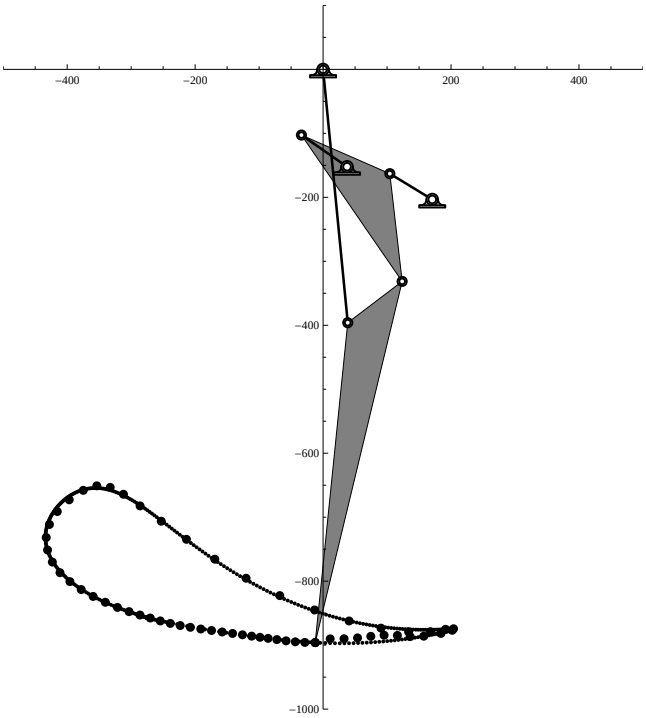

(b) Optimized linkage solution at the first precision point

Fig. 9: Optimized Stephenson III linkage solutions that have the largest variance from each other

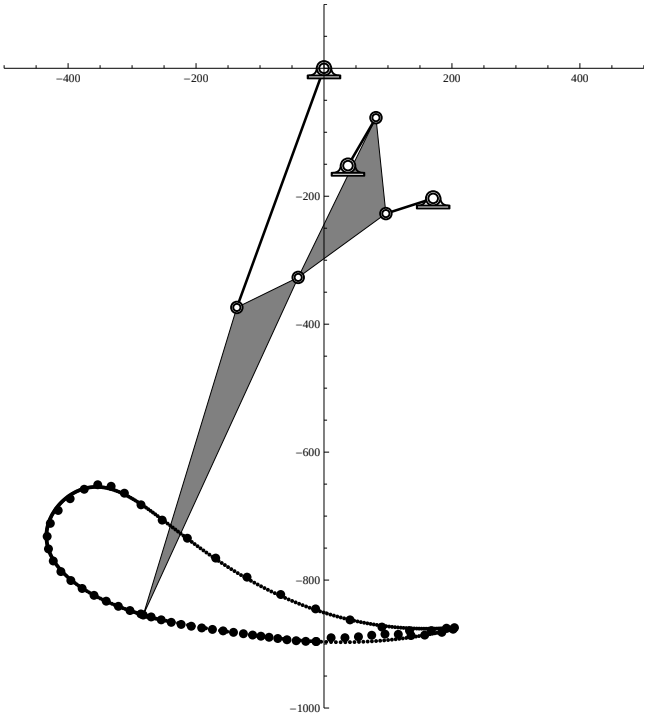

Fig. 10: One of 6 optimized linkage solutions in a position with a slightly hyper-extended knee joint

Fig. 11: Solidworks model of the optimized linkage solution

mation given from the motion capture data. All of these functions caused resulted in a convergence to the same solution. The resulting linkage created a desirable ankle trajectory, but caused the knee joint to extend to an undesirable angle.

After an analysis of the various optimization algorithms, it was observed that a particular starting position did not necessarily converge to the same solutions. For this reason, the use of the six different algorithms was used to provide a larger array of linkage solutions candidates. The result, after sorting the solution set, was 6 viable linkage solutions that created a desirable ankle trajectory and motion of the original 2R chain. These solutions were all in the same cluster. This research shows that the combination of optimization and algebraic methods can be used to find linkage solutions to guide the cyclic trajectory of an ankle during walking. It also shows how dependent optimization algorithms are on

starting positions and that using solutions found from homotopy methods can be a useful tool in selecting these starting values.

Acknowledgements

This material is based upon work supported by the National Science Foundation under Grant No. CMMI 1066082.

References

[1] Emken, J. L., Wayne, J. H., Harkema, S. J., and Reinkensmeyer, D. J., 2006. "A robotic device for manipulating human stepping". *IEEE Transactions on Robotics,* **22**(1), February, pp. 185–189.

[2] Kempe, A. B., 1876. "On a general method of describing plane curves of the nth degree by linkwork". *Proceedings of the London Mathematical Society,* **7**(1), pp. 213–216.

[3] Kapovich, M., and Milson, J., 2002. "Universality theorems for configuration spaces of planar linkages". *Topology,* **41**(6), pp. 1051–1107.

[4] Artobolevskii, I. I., 1964. *Mechanisms for the Generation of Plane Curves (Trans. R.D. Wills)*. Pergamon Press, Oxford.

[5] H. S. Kim, S. H., and Soni, A. H., 1971. "Synthesis of six-link mechanisms for point path generation". *Journal of Mechanisms,* **6**, April, pp. 447–461.

[6] Bhatia, D. H., and Bagci, C., 1977. "Optimum synthesis of multiloop planar mechanisms for the generation of paths and rigid-body positions by linear partition of design equations". *Journal of Engineering for Industry*, February, pp. 117–123.

[7] Nolle, H., 1975. "Linkage coupler curve synthesis: A historical review-iii. spatial synthesis and optimization". *Mechanism and Machine Theory,* **10**, pp. 41–55.

[8] Root, R. R., and Ragsdell, K. M., 1975. "A survey of optimization methods applied to the design of mechanisms". In Proceedings of the ASME Design Engineering Technical Conference, 75-DET-95.

[9] Mehdigholi, H., and Akbarnedjad, S., 2012. "Optimization of watt's six-bar linkage to generate straight and parallel leg motion". *International Journal of Advanced Robotic Systems,* **9**(22), pp. 1–6.

[10] Storn, R., and Price, K., 1997. "Differential evolution – a simple and efficient heuristic for global optimization over continuous spaces". *Journal of Global Optimization,* **11**, pp. 341–359.

[11] Bulatovic, R. R., and Dordevic, S. R., 2012. "Optimal synthesis of a path generator six-bar linkage". *Journal of Material Science and Technology,* **26**(12), July, pp. 4027–4040.

[12] Bulatovic, R. R., Dordevic, S. R., and Dordevic, V. S., 2013. "Cuckoo search algorithm: A metaheuristic approach to solving the problem of optimum synthesis of a six-bar double dwell linkage". *Mechanism and Machine Theory,* **61**, pp. 1–13.

[13] Dibakar, S., and Mruthyunjaya, T. S., 1999. "Synthesis of workspaces of planar manipulators with arbitrary topology using shape representation and simulated annealing". *Mechanism and Machine Theory,* **34**, pp. 391–420.

[14] McDougall, R., and Nokleby, S., 2008. "Synthesis of grashof four-bar mechanisms using particle swarm optimization". In Proceedings of the ASME International Design Engineering Technical Conferences and Computers and Information in Engineering Conference, DETC2008-49631.

[15] Xiao, R., and Tao, Z., 2005. "A swarm intelligence approach to path synthesis of mechanisms". In Proceedings of the IEEE 9th International Conference on Computer Aided Design and Computer Graphics.

[16] Smaili, A., and Diab, N., 2007. "Optimum synthesis of hybrid-task mechanisms using ant-gradient search method". *Mechanism and Machine Theory,* **42**, pp. 115–130.

[17] Bates, D. J., Hauenstein, J. D., Sommese, A. J., and Wampler, C. W., 2010. "Bertini: Software for numerical algebraic geometry". *http://www.nd.edu/ sommese/bertini*.

[18] Plecnik, M. M., and McCarthy, J. M., 2015. "Design of stephenson linkages that guide a point along a trajectory". *Mechanism and Machine Theory*, Submitted April.

[19] Plecnik, M. M., and McCarthy, J. M., 2015. "Computational design of stephenson 2 six-bar function generators for 11 accuracy points". *Journal of Mechanisms and Robotics*, Accepted for publication July.

[20] Unruh, V., and Krishnaswami, P., 1995. "A computer-aided design technique for semi-automated infinite point coupler curve synthesis of four-bar linkages". *Journal of Mechanical Design,* **117**, March, pp. 143–149.